Chapter 19
Comparison of Modal Parameters Extracted Using MIMO, SIMO, and Impact Hammer Tests on a Three-Bladed Wind Turbine

Javad Baqersad, Peyman Poozesh, Christopher Niezrecki, and Peter Avitabile

Abstract As part of a project to predict full-field dynamic strain of rotating structures (e.g. wind turbines or helicopter rotors), a validated numerical model of a structure is required. In this case, a small wind turbine was used. To understand the dynamic characteristics and validate a finite element model of a three-bladed wind turbine, several experimental modal analysis tests were conducted on the turbine attached to a 500-lb steel block. The test structure consisted of three 2.3-m blades mounted to a hub that was attached to the block using a shaft and a lathe chuck. In three separate tests, the structure was excited using a single shaker, multiple shakers, and an impact hammer; the responses of the structure to the excitations were measured using 12 triaxial accelerometers. The results reveal several very closely spaced modes present within the turbine in the test configuration. The natural frequencies and mode shapes obtained by using three different methods were compared to demonstrate the differences (e.g. strengths and weaknesses) between each excitation technique. The paper reports the results obtained and lessons learned during the experimental modal tests of the wind turbine.

Keywords Experimental modal analysis • Mode shape • Wind turbine • Multiple shakers

19.1 Introduction

Experimental modal analysis is extensively used to describe the dynamic characteristics of structures and to validate numerical models. Furthermore, these extracted modal parameters from the modal analyses are essential parts of many health-monitoring algorithms. Several experimental techniques are used to excite structures and to extract their modal parameters. Multiple-input multiple-output (MIMO) measurement, single-input multiple-output (SIMO) measurement, and impact hammer modal testing are three conventional approaches for experimental modal analysis. These three techniques may not always produce similar results if they are used for large complicated structures. Therefore, comparing the extracted parameters from these three techniques is desirable.

Modal impact hammer has been commonly used to extract the dynamic characteristics of wind turbine blades or wind turbine assemblies [1–7]. However, MIMO technique has been usually used for large structures such as a satellite [8] and inflatable torus [9]. A comparison between the MIMO and SISO (single-input single-output) results for a measurement on a membrane mirror satellite has been performed by Ruggiero et al. [10]. On the other hand, the number of studies found in the literature that compares the modal parameters estimated by using the three methods for a wind turbine that includes several subcomponents and has closely spaced modes is limited.

In the current paper, modal parameters extracted using MIMO, SIMO, and impact hammer modal techniques are compared to identify the differences between each excitation technique. The test structure, an assembled wind turbine, consisted of several substructures and has very closely spaced modes (less than 0.1 Hz difference). Therefore, the potential of each experimental modal approach in extracting the modal parameters of the structure can be examined. The current paper also summarized the results obtained and lesson learned during the experimental modal test of the wind turbine attached to a steel block.

J. Baqersad (✉) • P. Poozesh • C. Niezrecki • P. Avitabile
Structural Dynamics and Acoustic Systems Laboratory, University of Massachusetts Lowell,
One University Avenue, Lowell, MA 01854, USA
e-mail: javad_baqersad@student.uml.edu

R. Allemang (ed.), *Topics in Modal Analysis II, Volume 8: Proceedings of the 32nd IMAC, A Conference and Exposition on Structural Dynamics, 2014*, Conference Proceedings of the Society for Experimental Mechanics Series,
DOI 10.1007/978-3-319-04774-4_19,

19.2 Theoretical Background

19.2.1 Shaker Test with the Input Oblique to the Global Coordinate System

Often for convenience, shakers are installed in a direction parallel to one of the axes of the global coordinate system (X, Y, or Z) for SIMO or MIMO tests. The measured acceleration and force at the impedance head (as a reference) are required to properly obtain the frequency response functions of the structure at all the measurement points including the reference point to extract the mode shapes. However, installing a shaker parallel to an axis of the coordinate system does not excite the modes of the structure that have no component along that axis. For the current work, shakers were installed normal to the contact surface of the blade (at attached points) and oblique to the global coordinate system. For this setup, the direction of the input force and measured acceleration at an impedance head mounted to the shaker stinger cannot be defined using a single component of the global coordinate system (X, Y, or Z direction). Furthermore, finding the accurate orientation of the input force can be a challenge. Therefore, identifying an approach to easily orient the shakers in arbitrary configurations to conduct a modal test would be of particular interest [11]. The approach to extract the mode shapes when a shaker is installed in an oblique orientation is now described.

Experimental modal tests are performed to measure the frequency response functions of structures. The frequency response function (FRF) for a structure (i.e. the system transfer function evaluated in the frequency domain) can be defined as:

$$\mathrm{h_{ij}}\left(\mathrm{j}\omega\right) = \sum_{\mathrm{k}=1}^{\mathrm{m}} \frac{\mathrm{a_{ijk}}}{\left(\mathrm{j}\omega - \mathrm{p_k}\right)} + \frac{\mathrm{a_{ijk}^*}}{\left(\mathrm{j}\omega - \mathrm{p_k^*}\right)} \tag{19.1}$$

where, p_k is the k-th mode of the system. Residues (a_{ijk}) can be calculated using the following equation:

$$\mathrm{a_{ijk}} = \mathrm{q_k u_{ik} u_{jk}} \tag{19.2}$$

where u_{ik} and u_{jk} are the k-th mode of the structure at point i and j respectively. As can be seen, the residues are directly related to the system mode shapes and are scaled by q_k, the scaling constant for k-th mode. The residue matrix for the whole set of measurement can be written as:

$$\begin{bmatrix} \mathrm{a_{11k}} & \mathrm{a_{12k}} & \mathrm{a_{13k}} & \cdots \\ \mathrm{a_{21k}} & \mathrm{a_{22k}} & \mathrm{a_{23k}} & \cdots \\ \mathrm{a_{31k}} & \mathrm{a_{32k}} & \mathrm{a_{33k}} & \cdots \\ \vdots & \vdots & \vdots & \ddots \end{bmatrix} = \mathrm{q_k} \begin{bmatrix} \mathrm{u_{11k}} & \mathrm{u_{12k}} & \mathrm{u_{13k}} & \cdots \\ \mathrm{u_{21k}} & \mathrm{u_{22k}} & \mathrm{u_{23k}} & \cdots \\ \mathrm{u_{31k}} & \mathrm{u_{32k}} & \mathrm{u_{33k}} & \cdots \\ \vdots & \vdots & \vdots & \ddots \end{bmatrix} \tag{19.3}$$

If a particular reference such as *10y* (where the shaker is installed) is picked for the measurement, the set of data for a single reference can be written as:

$$\begin{Bmatrix} \mathrm{a_{1x10y}} \\ \mathrm{a_{1y10y}} \\ \mathrm{a_{1z10y}} \\ \mathrm{a_{2x10y}} \\ \mathrm{a_{2y10y}} \\ \vdots \\ \mathrm{a_{10y10y}} \\ \vdots \\ \mathrm{a_{40y10y}} \\ \mathrm{a_{40z10y}} \end{Bmatrix} == \mathrm{qu_{10y}} \begin{Bmatrix} \mathrm{u_{1x}} \\ \mathrm{u_{1y}} \\ \mathrm{u_{1z}} \\ \mathrm{u_{2x}} \\ \mathrm{u_{2y}} \\ \vdots \\ \mathrm{u_{10y}} \\ \vdots \\ \mathrm{u_{40y}} \\ \mathrm{u_{40z}} \end{Bmatrix} \tag{19.4}$$

where, points 1–40 are measurement points. The drive point measurement (point *10y*) is used to scale the residues to get the scaled mode shapes for all the measurement points including the drive point.

$$\mathrm{a_{10y10y}} = \mathrm{qu_{10y} u_{10y}} \tag{19.5}$$

However, the structure can be excited using an oblique shaker to excite more modes of the system that might not be excited by a single shaker in *y*-direction. If the input force excites the system at point *41* and is orientated in an unknown direction called s, the set of data for a particular mode can be written as:

$$\begin{Bmatrix} a_{1x41s} \\ a_{1y41s} \\ a_{1z41s} \\ a_{2x41s} \\ a_{2y41s} \\ \vdots \\ a_{10y41s} \\ \vdots \\ a_{40y41s} \\ a_{40z41s} \\ a_{41s41s} \end{Bmatrix} = qu_{41s} \begin{Bmatrix} u_{1x} \\ u_{1y} \\ u_{1z} \\ u_{2x} \\ u_{2y} \\ \vdots \\ u_{10y} \\ \vdots \\ u_{48y} \\ u_{48z} \\ u_{41s} \end{Bmatrix} \tag{19.6}$$

and the drive point measurement is:

$$a_{41s41s} = qu_{41s}u_{41s} \tag{19.7}$$

Equation (19.7) can be used to scale the mode shape for points *1* to *40* in Eq. 19.6. However, once the mode shapes are scaled using the drive point measurement, point *41* can be excluded from the mode shape description. Thus, the mode shape of the structure can be extracted without identifying the orientation of the input force. The same procedure can be repeated for a MIMO measurement. This means that for the mode shape description, no geometric point exists at drive points (impedance heads).

19.3 Structure Description and Test Setup

As part of a project to predict full-field dynamic strain for a rotating structure and in order to validate a finite element model, an experimental modal measurement on a wind turbine in a fixed condition needed to be performed. In order to prepare a test set up for the wind turbine, three blades of a Southwest Windpower Skystream 4.7 were mounted to a central hub while connected to a 500-lb block using a lathe chuck and a shaft. The 2.3-m blades were made of a composite/plastic material. The hub included an aluminum component and a steel plate that were connected using 12 steel bolts. In order to isolate the vibration of the block from the ground and to prevent rattling along the contact surface, some layers of elastic foam were used. A photograph of the test set-up is shown in Fig. 19.1. Although different excitation techniques (three-shaker, single-shaker, and an impact hammer) were used for Cases 2–4, the test configuration and measurement steps were similar for all three cases and are now described.

The location of the sensors was selected using a finite element (FE) model of the wind turbine. By performing an eigensolution on the numerical model in a fixed boundary condition, FE mode shapes were extracted. Using the FE model, an appropriate set of sensor locations was selected so that all the modes of interest could be identified (see Fig. 19.2). The origin of the coordinate system for the turbine is located at the center of the hub where X-axis and Z-axis are in the rotating plane and Z points toward the tip of Blade 1 (see Fig. 19.2). The Y-axis refers to the transverse displacement of the blade (i.e. the out-of-plane or flapwise direction).

A 60-channel LMS data acquisition system was used to record the response of the structure and the input force. Because extracting both flapwise and edgewise modes were desirable, triaxial accelerometers were selected for the testing. Twelve accelerometers were mounted per blade distributed at locations over all three blades of the turbine. The frequency bandwidth of the acquisition system for all the measurements (Cases 1–4) was 128 Hz; however, due to spatial resolution, only the results below 80 Hz are shown in the current paper (mode shapes with natural frequencies higher than 80 Hz have curvatures that are difficult to show with the limited number of measurement points).

The limitations in the number of available accelerometers and the available channels of the data acquisition system did not allow all the measurements to be carried out in a single set-up of accelerometers. Therefore, the test was performed on four

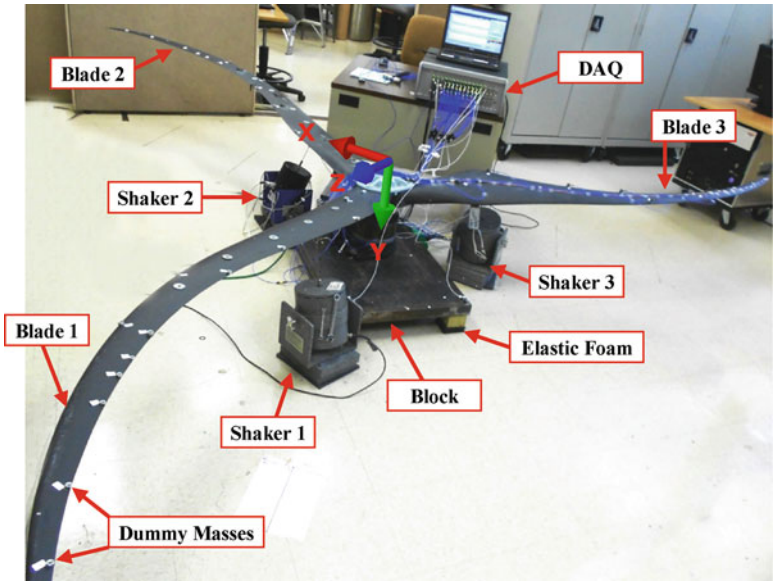

Fig. 19.1 A photograph of the test set-up showing the wind turbine attached to the steel-block (the accelerometers are mounted to Blade 3)

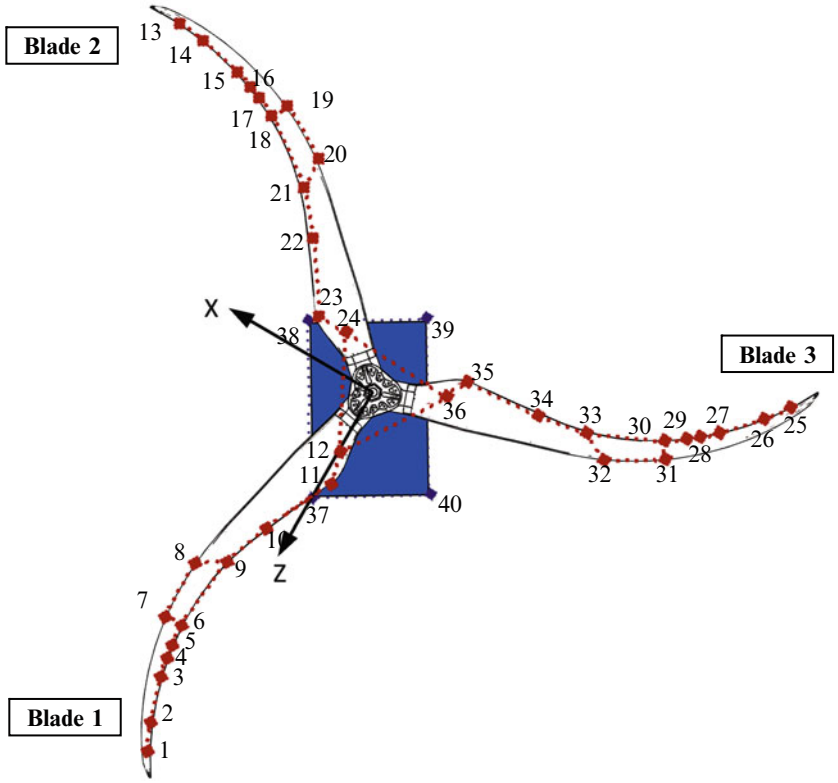

Fig. 19.2 A drawing of the test set-up showing the sensor locations

separate set-ups; however, this requires extra consideration to mass loading which is discussed further. For the first set-up, all the accelerometers were installed on Blade 1. The response of the turbine to the excitations was measured by using 12 triaxial accelerometers mounted to Blade 1 (36 channels). Then, the accelerometers were moved to Blade 2 and the response of the structure was measured. Next, the accelerometers were moved to Blade 3 and same measurements were repeated. The final set of measurement was performed when four of the triaxial accelerometers were attached to the support block and the turbine was exited by using impact hammers or shakers.

To compensate for the mass of the accelerometers, dummy masses were installed to emulate the weight of the accelerometers and connected wires. When the accelerometers are mounted to one blade, a set of dummy masses were used

on the accelerometer locations of the other two blades. In order to lower the mass loading effects, lighter accelerometers were used at the points near the tip of the blades. (The use of dummy masses on this type of lightweight blade structure is critical to the success of measuring and extracting useful mode shapes. If these compensation masses are not used then there would be a significant mass loading effect and the frequency response functions used for the modal extraction process would not be of sufficient quality to extract accurate mode shapes).

19.4 Test Cases Studied

19.4.1 Case 1: Impact Hammer Modal Test on the Fixture

The primarily objective of the work was to find the mode shapes of the wind turbine in a fixed configuration. However, providing a test condition for the turbine that replicates the built-in condition is very difficult. Considering the available equipment, the turbine was attached to a fixture that included a lathe chuck and a steel block placed on layers of elastic foam. However, some modes of the fixture might occur in the bandwidth of interest (the bandwidth that was used to extract the modes of the turbine in fixed condition). Therefore, due to interactions between the modes of the fixture and the wind turbine, the modes of the fixture needed to be determined before the fixture was attached to the turbine.

In order to identify the modes that were associated with the test rig, a modal impact hammer test was performed on the fixture alone (see Fig. 19.3). The purpose of this test was to understand the contribution of the test fixture to the overall dynamics of the complete turbine blade attached to the test fixture. On the other hand, the set up needed to consider the inertial effects of the turbine but not their mode shapes. In order to emulate the inertia effects of the blades, some masses were mounted to the shaft. Due to limitation in mountings, the added mass could partially replicate the masses of the blades (the added mass is only 11 kg while the mass of the turbine was 23 kg). Likewise, the rotational inertia effect of the turbine blades (that is due to off-center distribution of the mass of the blades) was not considered in this set up. These effects might cause some discrepancies between the modes extracted in this case and fixture modes extracted when the blades are also attached to the fixture; this will be addressed in Case 2 when the fixture modes are described.

Using four triaxial accelerometers, a modal impact hammer test was performed on the structure. Because, the flexible modes of the plate were in higher frequencies than the frequency bandwidth of interest, accelerometers were only mounted to the corners of the block. Figure 19.4 shows sample FRF and coherence plots of the measurement. The six modes of the structure extracted using a LMS PolyMAX [12] stability diagram are shown in Fig. 19.5.

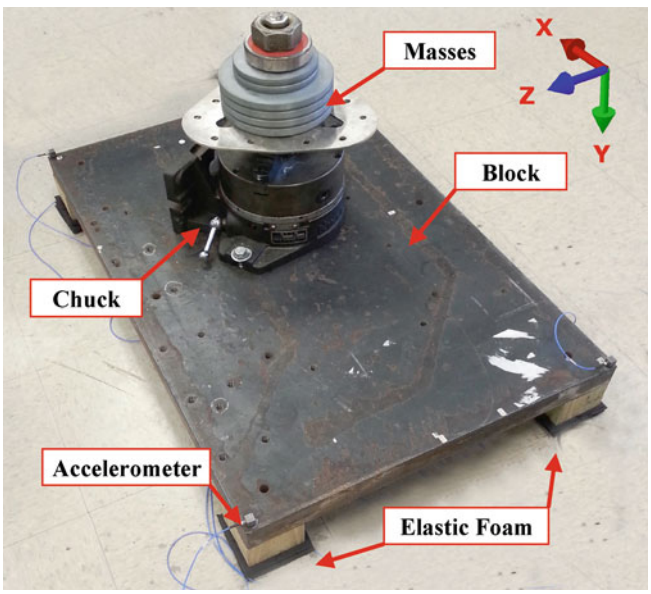

Fig. 19.3 A photograph of the fixture showing the chuck, masses, and 500-lb block placed on layers of elastic foam

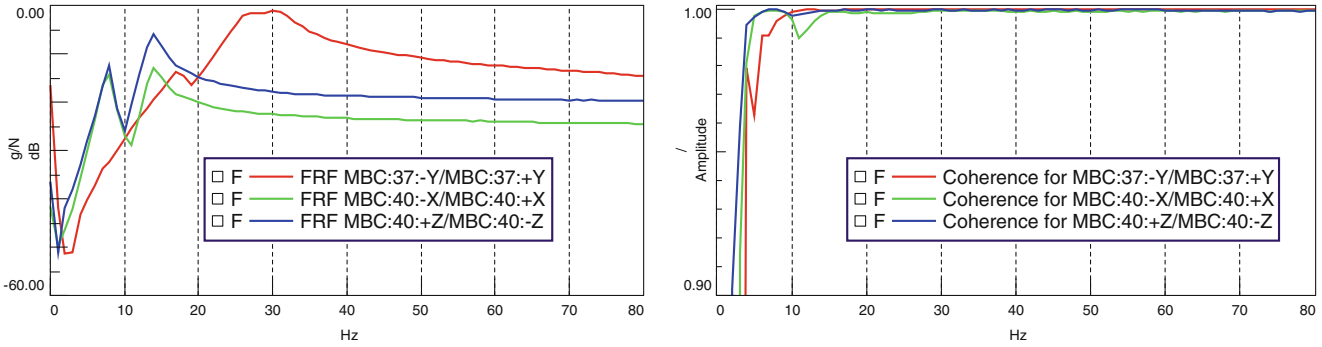

Fig. 19.4 Sample FRF and coherence plots for the impact test measurement on the fixture

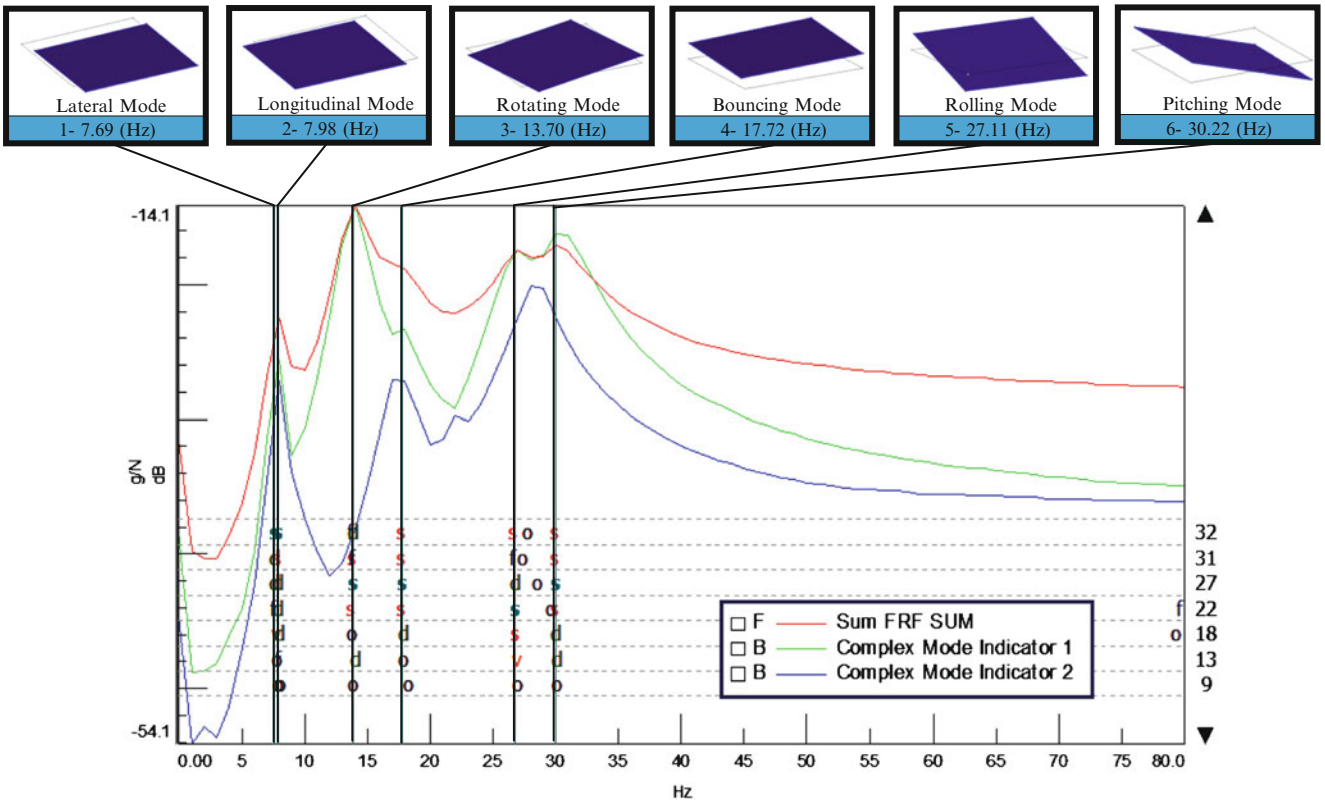

Fig. 19.5 Stability diagram, natural frequencies, and mode shapes of the fixture (500-lb block and accessories) on layers of elastic foam

19.4.2 Case 2: MIMO Test on the Wind Turbine Assembly

A MIMO test was performed on the structure using three shakers (see Fig. 19.1). Each shaker was connected to a single blade and was exciting the turbine using a burst random input. Because there were very closely spaced modes in the structure, a high resolution was used for the data acquisition (1,024 spectral lines that needed 8 s of data recording). Before performing the measurement, a principle component analysis was performed to assure that all three shakers were uncorrelated and independent.

In order to identify the resonant frequencies of the assembly, a LMS PolyMAX [12] stability diagram was used. Figure 19.6 shows the natural frequencies and mode shapes of the wind turbine attached to the steel block. The color code shows the grouping of the modes.

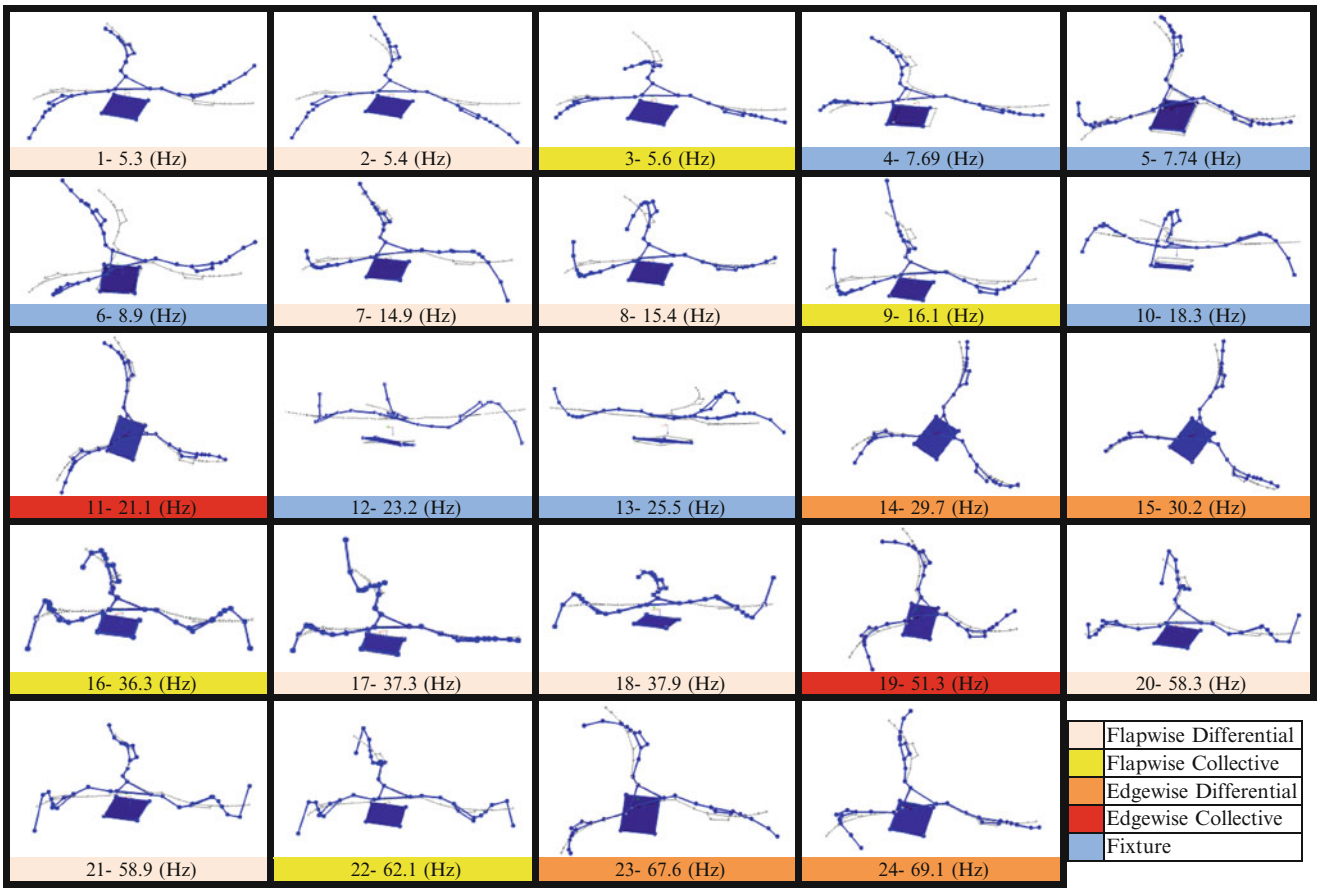

Fig. 19.6 Natural frequencies and mode shapes of the wind turbine attached to the 500-lb block

The modes of the assembled structure that come from the modes of the test setup are called fixture modes in Fig. 19.6. These modes were identified by comparing their shapes and frequencies to the modes shown in Fig. 19.5. Comparing the results in Figs. 19.5 and 19.6, the natural frequencies for the modes of the test rig that were related only to the mass of the structure (modes 4, 5, and 10 in Fig. 19.6 that are respectively equivalent to lateral, longitudinal, and bouncing modes shown in Fig. 19.5) have slightly changed. However, the modes of the structure that were related to the rotational inertia of the assembly (modes 6, 12, and 13 in Fig. 19.6 that are respectively equivalent to rotating, rolling, and pitching modes shown in Fig. 19.5) show a significant change. This can be attributed to the fact that in the model shown in Fig. 19.2, the effect of the distributed mass of the turbine that would influence the rotational inertia of the structure was not considered.

The modes of a turbine can be categorized as either collective or differential modes. The collective modes are the modes with the same phase on three blades; the differential modes are the modes that the blades do not have the same phase or deflection.

19.4.3 Case 3: SIMO Test on the Wind Turbine Assembly

In the SIMO test, the test set up shown in Fig. 19.1 was used; however, only Shaker 1 was exciting the structure. The data acquisition system used the same set-up as previous measurement in Case 2. Most of the modes of the assembled structure that were shown in Fig. 19.6 could be extracted by the SIMO measurement. A comparison between the modal parameters extracted using MIMO, and SIMO measurement techniques is performed in the Sect. 19.5 of the paper.

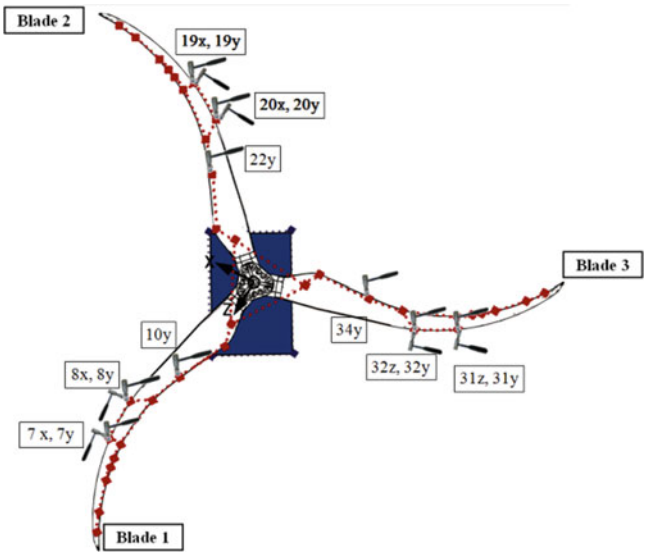

Fig. 19.7 A drawing of the turbine showing the impact locations/orientations for the modal impact hammer test (Y-axis shows out of plane; X-axis and Z-axis show in-plane impacts)

19.4.4 Case 4: Modal Impact Hammer Test on the Wind Turbine Assembly

Modal impact hammer test was also performed on the structure. For this measurement, the blades were excited in 15 locations/orientations as shown in Fig. 19.7 using a modal impact hammer with a rubber tip. The force impacts were made both in flap and edge directions. The data acquisition system was used with the same set up as the previous cases (frequency bandwidth of 128 and 1,024 Hz spectral lines). The extracted modal parameters are presented in the Sect. 19.5.

19.5 Discussion

19.5.1 Discussion 1: MIMO–SIMO Comparison

As previously described, the modes of the structure were extracted using MIMO and SIMO techniques in two separate tests. In this section, a comparison between the FRFs extracted with these methods is performed.

To study the differences of the results when the structure is excited with multiple shakers and a single shaker, the measured FRFs at a measurement point located at the tip of the Blade 1 for MIMO and SIMO tests are shown in Fig. 19.8. As can be seen, the measured FRF for the MIMO test due to Shaker 1 and the measured FRF for the SIMO test overlap very well. That occurs because for the SIMO test, only Shaker 1 (attached to Blade 1 where the measured point is located) was exciting the structure. The FRF measured for the MIMO test due to excitation by Shakers 2 and 3 are also shown in Fig. 19.8. These FRFs reveal that some modes of the system have better been excited by using Shakers 2 and 3 rather than Shaker 1. For instance, the two modes of the system that were located near 8 Hz can be more clearly found in the excitation by Shakers 2 and 3 than Shaker 1 (see Fig. 19.8). Therefore, modes of the system were more effectively excited for a MIMO test rather than a SIMO test; that would lead to extracting more accurate FRFs for the MIMO test.

For a comprehensive comparison between the measured FRFs using two techniques, three measured FRFs from the MIMO test due to Shaker 1 and SIMO test (that is also due to Shaker 1) and their corresponding coherences are overlaid in Fig. 19.9. The FRFs related to the measurement points at the tip of the three blades for x and y directions. As can be seen, the FRFs for point *1y* (i.e. the tip of the Blade 1 at the flap direction) compare very well for two techniques. It should be noted that for the SIMO test, the only shaker that was exciting the system (Shaker 1) was connected to Blade 1; this might describe why the measured FRFs at tip of that Blade 1 for MIMO and SIMO tests are very similar. However, the FRFs for the tip of the Blade 2 (Fig. 19.9 middle curve) do not compare as well as the tip of the Blade 1. This might be attributed to the fact that an energy loss occurred when the energy was transmitted through the hub and connections. In addition, this might be also attributed the shaker stingers; in the MIMO test the effect of the stingers is symmetrical while in SIMO test is not. As can be

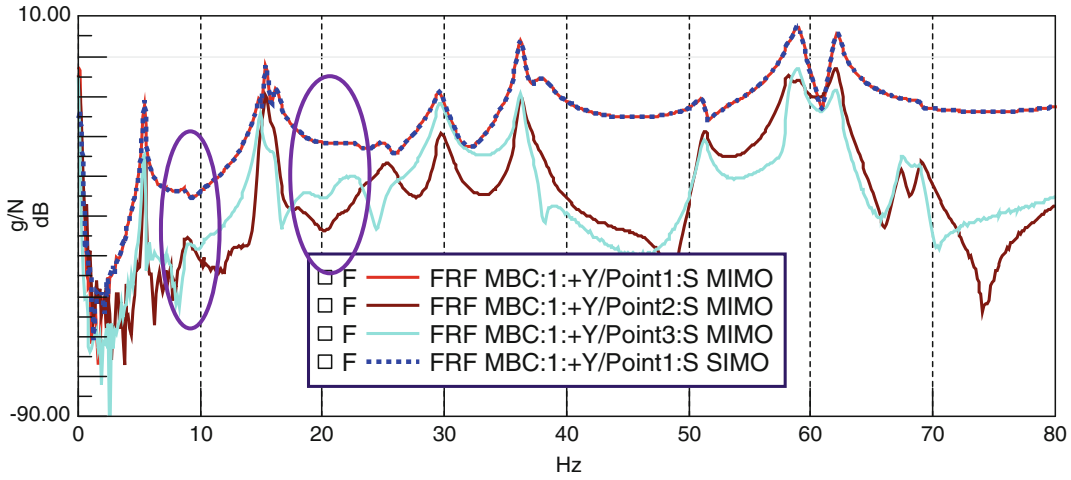

Fig. 19.8 A comparison between the FRF for the tip point of Blade 1 due to different shakers for the MIMO test and due to the single shaker for the SIMO test (MBC: 1 is the tip of the Blade 1 and Points 1, 2, and 3 are the points that shakers are connected to Blades 1, 2, and 3 respectively); the *ovals* show the modes that have better been excited with shakers on Blades 2 and 3 rather than shaker installed on Blade 1

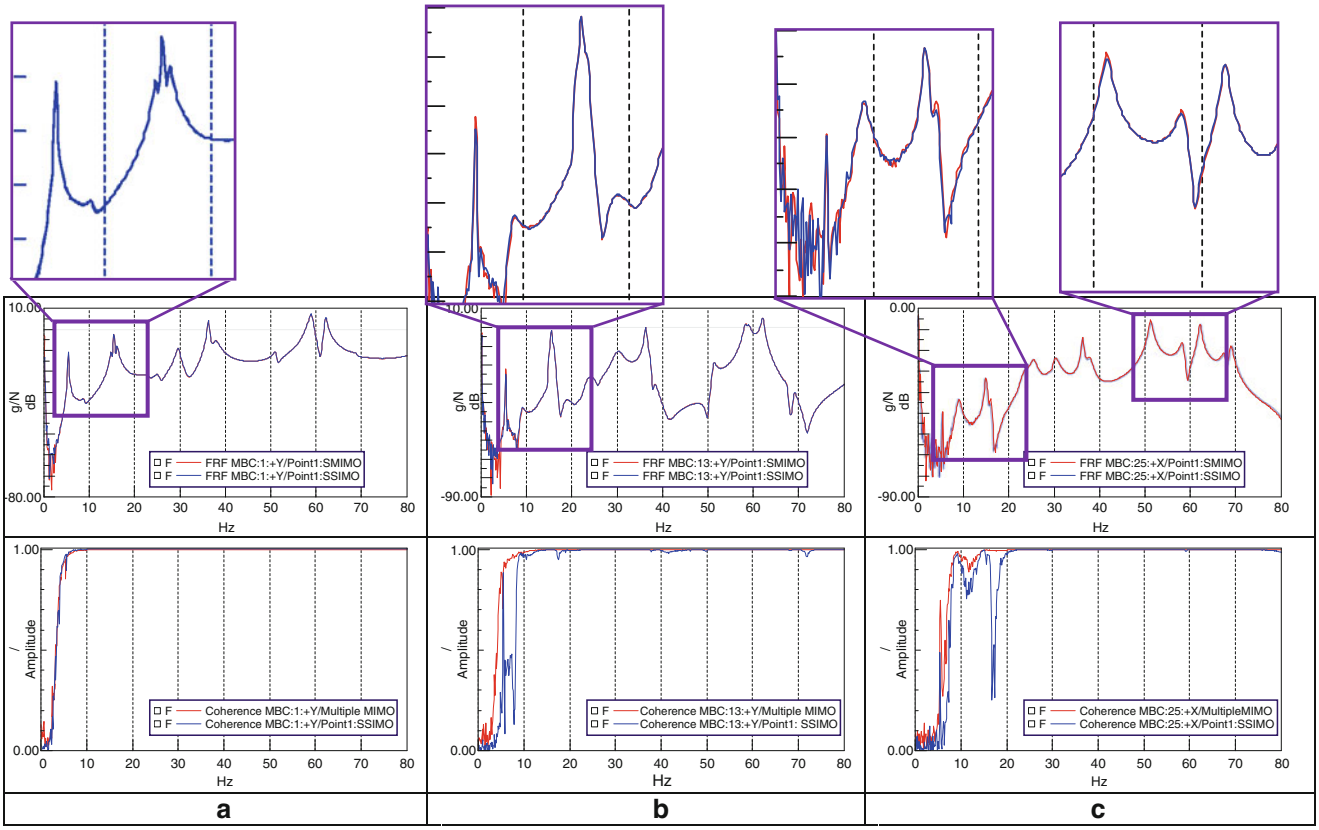

Fig. 19.9 Comparisons between the FRF and coherence for the MIMO and SIMO tests for different locations/orientations, (**a**) measured FRF and coherence at the tip of the Blade 1 in the y direction due to shaker excitation attached to Blade 1, (**b**) measured FRF and coherence at the tip of the Blade 2 in the y direction due to shaker excitation attached to Blade 1, (**c**) measured FRF and coherence at the tip of the Blade 3 in the x direction due to shaker excitation attached to Blade 1

seen, the coherence of this measurement for the SIMO test is not at the same quality as that for the MIMO test. If the FRFs are measured for the points that do not have large deflections in the modes, the measured FRFs show a higher difference. As can be seen in Fig. 19.9 right plot, the measured FRFs for x direction show higher deviations between the two methods and the coherence for the SIMO test is not as good as the MIMO test.

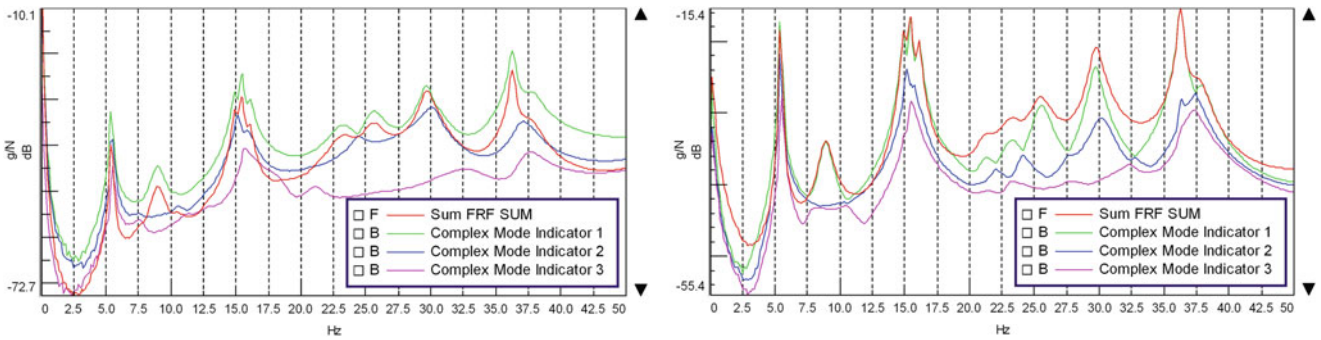

Fig. 19.10 Summation and complex mode indicator functions of the measure FRFs for the MIMO test (*left*) and the impact hammer modal test (*right*); the *ovals* indicate modes that can be seen more distinctly using impact test rather than MIMO test

19.5.2 Discussion 2: Location of the Shakers

Selecting the location and orientation of the shaker is an important part of SIMO and MIMO measurements. A poor selection of the reference points may lead to weak representation of the mode shapes. A proper selection of the reference points, however, excites the desirable modes of the structure. Preferably, a shaker should be attached to a point that the mode shapes show a high value at (far from nodes of the modes). On the other hand, although the tips of the blades show high deflections for most of the modes, the shakers cannot be attached to those points because the shaker may not be able to generate the necessary displacement at these points during excitation. Therefore, the shakers were attached to the structure at points near the root of the blade. In fact, the drive points were located approximately 60 cm far from the center of the turbine so they can excite the first three flapwise modes of the turbine (the node of the first flapwise and edgewise modes of the single blades are near the root of the blades). Furthermore, by using an oblique installation of the shakers, both flapwise and edgewise modes of the structure could be excited.

In order to demonstrate the effects of the location and orientation of the shakers on exciting the modes of the structure, the stability diagram of the structure for the measured FRFs during MIMO test (Fig. 19.10, left) is compared to impact hammer test (Fig. 19.10, right). The modes of the structure can be identified by the peaks in the plot. As can be seen, there are some modes of the structure that have not been effectively excited for the MIMO test while for the impact test (Fig. 19.10, right) those peaks can be seen more distinctly. This occurs because of the location and orientation of the shakers. The shakers could excite the first three flapwise modes of the blades at approximately 5.5 Hz. However, the first edgewise modes of the blades could not be effectively excited (at approximately 21.1 Hz) because the stiffness of the blades in edge direction was much higher than the flapwise direction. Moreover, the shakers are more inclined toward the flap direction than edge direction because extracting flapwise modes were considered more important. Therefore, if a better representation of the edgewise modes were needed, the shakers would have to be installed far from the roots and more oblique toward the edge direction (it should be noted that installing the shakers close to tip of the blade is also a challenge because of the high flexibility of the blade near the tip). The impact hammer modal test, however, shows a clear peak at the frequency of the first edgewise mode of the turbine. This occurs because for the impact test, the force edgewise impacts could be made at points that were far from the hub. When the force is applied to the turbine at points far from the hub, the edgewise modes of the structure can be efficiently excited.

19.5.3 Discussion 3: Comparing the Modal Parameters Extracted using SIMO, MIMO, and Impact Tests

In this section, a comparison between the MIMO and SIMO tests along with a comparison between MIMO and impact tests are performed. The correlation shows the percentage of change in natural frequency and damping extracted using different techniques. The mode shapes are correlated using modal assurance criterion (MAC).

Table 19.1 shows a comparison between the MIMO and SIMO tests. The results show that for most of the modes, both of the techniques show similar results. A strong correlation between the results for the first mode extracted using the two methods can be seen. However, modes 2 and 3 do not show strong correlations. This can be attributed to the fact that usually MIMO test can have better distribution of energy over the structure. On the other hand, the location and orientation of the

Table 19.1 Correlation between extracted modal parameters for MIMO and SIMO tests

	MIMO test		SIMO test		Correlation		
Mode #	Freq. (Hz)	Damp. (%)	Freq. (Hz)	Damp. (%)	Freq. diff. (%)	MAC (%)	
1	5.3	0.9	5.3	0.7	0.6	97.0	
2	5.4	0.7	5.4	0.9	0.2	81.9	
3	5.6	0.5	5.6	0.3	0.3	78.0	
4	7.7	5.4	–	–	N/A	N/A	Fixture mode
5	7.7	3.6	–	–	N/A	N/A	Fixture mode
6	8.9	4.8	8.9	4.5	0.3	98.4	Fixture mode
7	14.9	1.3	14.9	1.2	0.0	99.3	
8	15.4	0.7	15.4	0.8	0.0	99.9	
9	16.1	1.3	16.1	1.4	0.0	99.8	
10	18.3	5.8	18.5	2.9	1.2	28.8	Fixture mode
11	21.1	3.3	21.0	2.2	0.8	47.7	
12	23.2	4.5	23.2	4.1	0.0	97.9	Fixture mode
13	25.5	2.8	25.5	2.7	0.1	99.0	Fixture mode
14	29.7	1.5	29.7	1.5	0.0	99.3	
15	30.2	3.1	30.2	3.1	0.1	98.0	
16	36.3	0.6	36.3	0.6	0.0	99.9	
17	37.3	2.4	37.4	2.3	0.3	92.6	
18	37.9	1.8	37.9	1.8	0.2	95.0	
19	51.3	0.7	51.2	0.7	0.1	99.7	
20	58.3	0.7	58.3	0.7	0.0	99.4	
21	58.9	0.7	58.9	0.7	0.0	99.7	
22	62.1	0.5	62.1	0.5	0.0	99.9	
23	67.6	0.6	67.5	0.6	0.0	91.2	
24	69.1	0.6	69.1	0.6	0.0	99.4	

shaker or the amount of energy imparted to the structure for SIMO test could not effectively excite the longitudinal, lateral, and bounce modes of the fixture (modes 4, 5, and 10); that is why these modes could not be identified for the SIMO test or they show a weak correlation. The weak correlation between the results for mode 11 also can be attributed to the improper excitation of that mode by a single shaker as could be predicted using the FRF in Fig. 19.8 (mode 11 is the first edgewise mode with a node located near the root of the blade).

A correlation between the modal parameters extracted using MIMO test and modal parameters extracted using impact test are shown in Table 19.2. The results of Table 19.2 show high correlations between the modes of the structure using these two methods. The first edgewise mode of the turbine also shows a high correlation. However, the lateral and longitudinal modes of the fixture (modes 4 and 5) could not be extracted using modal impact hammer method. This should be noted that although making impacts at the points of the blades far from the hub could efficiently excite the edgewise modes of the turbine (for those modes the turbine deforms along the hub axis and the hub is the nodes of these modes), these impacts did improve excitation of the transverse and lateral modes of the fixture. Moreover, the bouncing mode of the structure (mode 10) shows a weak correlation between two methods. These can be attributed to the fact that the small impact force applied by using the rubber head of the hammer could not excite the global modes of the structure. However, if a better representation of these modes were needed, some force impacts could have been made on the fixture with a bigger modal hammer.

Comparing the results of Tables 19.1 and 19.2, it is evident that the MIMO test results show a higher correlation to the impact hammer modal test rather than SIMO test. This can be attributed to the fact that for both MIMO and impact test measurements, a more uniform distribution of the input energy could be applied to all three blades. However, for the SIMO test, the input force was applied to the system through a single blade. Therefore, the energy might not be uniformly distributed for the entire structure.

19.6 Observation

In this section, several important lessons from the paper are pointed out that can be used in future measurements.

For Case 1, extracting modes of the fixture with considering the inertia of the blades was desirable. Therefore, to replicate the inertia of the blades, a lumped mass was added to the hub. However, the lumped mass could not mimic the rotational

Table 19.2 Correlation between extracted modal parameters for MIMO and impact hammer tests

	MIMO test		Impact hammer test		Correlation		
Mode #	Freq. (Hz)	Damp. (%)	Freq. (Hz)	Damp. (%)	Freq. diff. (%)	MAC (%)	
1	5.3	0.9	5.3	0.7	0.2	98.7	
2	5.4	0.7	5.4	0.6	0.0	99.5	
3	5.6	0.5	5.6	0.5	0.0	97.9	
4	7.7	5.4	–	–	N/A	N/A	Fixture mode
5	7.7	3.6	–	–	N/A	N/A	Fixture mode
6	8.9	4.8	8.9	4.9	0.8	98.6	Fixture mode
7	14.9	1.3	14.9	1.5	0.0	99.9	
8	15.4	0.7	15.4	0.7	0.0	99.9	
9	16.1	1.3	16.1	1.3	0.0	99.9	
10	18.3	5.8	18.9	2.8	3.2	22.0	Fixture mode
11	21.1	3.3	21.1	2.9	0.0	94.6	
12	23.2	4.5	23.3	4.1	0.2	98.4	Fixture mode
13	25.5	2.8	25.5	2.6	0.1	99.1	Fixture mode
14	29.7	1.5	29.7	1.5	0.1	99.5	
15	30.2	3.1	30.2	3.1	0.0	97.2	
16	36.3	0.6	36.2	0.6	0.1	99.9	
17	37.3	2.4	37.3	2.4	0.0	97.9	
18	37.9	1.8	37.9	1.8	0.2	98.9	
19	51.3	0.7	51.3	0.8	0.0	99.8	
20	58.3	0.7	58.3	0.7	0.0	99.5	
21	58.9	0.7	58.9	0.7	0.1	99.6	
22	62.1	0.5	62.1	0.5	0.1	99.9	
23	67.6	0.6	67.6	0.6	0.0	99.4	
24	69.1	0.6	69.1	0.3	0.1	99.9	

effects of the blades. After obtaining the modes of the assembly (Fig. 19.6), a considerable change in some modes of the fixture (Fig. 19.5) was seen. This change is more significant in the modes that are dependent to the rotational inertia of the blades. The results of this paper show the significant effects of rotational inertia on the structures where mass is distributed far from the rotation axis.

Another important lesson that can be learned from this measurement was the effects of impact locations on the extracted modes. For the impact test, if the measured FRFs for the case when impact forces are only made on a single blade were used, not all the modes could be extracted; this was observed in the results but was not presented in this paper due to space limitation. For instance, if the measured FRFs of the test when only Blade 1 was excited were used, mode 2 of the turbine could not be identified. Therefore, if the input force is distributed on all the components of a structure in a modal test, a better representation of the modes (or even more modes of the structure) can be extracted. This fact also clarifies why SIMO test results do not compare very well with the MIMO and impact tests. For SIMO test, the force was imparted to the turbine only through a single point and on a single blade; therefore, not all the modes might be effectively excited.

19.7 Conclusion

The results of the study revealed there are very closely space modes in the three-bladed turbine attached to the steel block. The modes of the assembled turbine were categorized into: (1) collective flapwise modes, (2) differential flapwise modes, (3) collective edgewise modes, (4) differential edgewise modes, and (5) fixture modes. In this paper, the technique for installing shakers in oblique orientations was implemented for a wind turbine blade; the modes of the structure could be found without the need for finding the installed angles of the shakers. Comparing the MIMO and SIMO results showed that a complicated structure such as a wind turbine that has several connections among the subcomponents needs to be excited by several shakers. Using multiple shakers leads to a uniform distribution of the energy over the entire structure and a better coherence in the measurement. On the other hand, a single shaker could not effectively excite all the modes of the structure. The results of the study also showed that impact hammer modal test is still one of the powerful techniques to excite structures for an experimental modal test. The results revealed that for a complicated structure with several substructures, impact hammer

modal test leads to better results rather than SIMO test. If only a few impact references are used and all of these references are located on one blade, then the results may not adequately represent the modes. However, if many impact reference locations are used on all three blades, then very good results can be obtained.

Acknowledgements This material is based upon work supported by the National Science Foundation under Grant Number 1230884 (Achieving a Sustainable Energy Pathway for Wind Turbine Blade Manufacturing). Any opinions, findings, and conclusions or recommendations expressed in this material are those of the author(s) and do not necessarily reflect the views of the National Science Foundation.

References

1. Paquette J, Laird D, Griffith DT, Rip L (2006) Modeling and testing of 9m research blades. In: 44th AIAA aerospace sciences meeting, vol 19, pp 14569–14581
2. Ye Z, Ma H, Bao N, Chen Y, Ding K (2001) Structure dynamic analysis of a horizontal axis wind turbine system using a modal analysis method. Wind Eng 25(4):237–248
3. LoPiccolo J, Carr J, Niezrecki C, Avitabile P, Slattery M (2012) Validation of a finite element model used for dynamic stress-strain prediction. In: 30th IMAC, a conference on structural dynamics, vol 2, pp 205–214
4. Deines K, Marinone T, Schultz R, Farinholt K, Park G (2011) Modal analysis and SHM investigation of CX-100 wind turbine blade. In: 29th IMAC, a conference on structural dynamics, vol 5, pp 413–438
5. Marinone T, LeBlanc B, Harvie J, Niezrecki C, Avitabile P (2012) Modal testing of 9 m CX-100 turbine blades. In: 30th IMAC, a conference on structural dynamics, vol 2, pp 351–358
6. Harvie J, Avitabile P (2012) Comparison of some wind turbine blade tests in various configurations. In: 30th IMAC, a conference on structural dynamics, vol 2, pp 73–79
7. Baqersad J, Niezrecki C, Avitabile P, Slattery M (2013) Dynamic characterization of a free-free wind turbine blade assembly. In: 31th IMAC, a conference on structural dynamics, pp 215–220
8. Avitabile P, Singhal R, Peeters B, Leuridan J (2005) Modal parameter estimation approaches for large complicated multiple reference tests (then and now). In: 23th IMAC, a conference and exposition on structural dynamics
9. Ruggiero EJ, Park G, Inman DJ (2004) Multi-input multi-output vibration testing of an inflatable torus. Mech Syst Signal Process 18(5): 1187–1201
10. Ruggiero EJ, Inman DJ (2005) A comparison between SISO and MIMO modal analysis techniques on a membrane mirror satellite. J Intell Mater Syst Struct 16(3):273–282
11. Avitabile P (2009) MODAL SPACE: if I run a shaker test with the input oblique to the global coordinate system, how do I decompose the force into the specific components in each direction? Exp Tech 33(5):11–12
12. [LMS Test.Lab 10A] (2009) LMS International, Leuven, Belgium